IMPACT OF COLLISION AVOIDANCE MANOEUVRES ON LARGE SATELLITE CONSTELLATIONS

Lucía Ayala Fernández[(1)], Jonas Radtke[(2)], and Enrico Stoll[(3)]

[(1)]*Technische Universität Braunschweig, 38108 Braunschweig, Germany, Email: l.ayala-fernandez@tu-braunschweig.de*
[(2)]*OKAPI:Orbits, 38108 Braunschweig, Germany, Email: jonas.radtke@okapiorbits.com*
[(3)]*Technische Universität Berlin, 10587 Berlin, Germany, Email: e.stoll@tu-berlin.de*

ABSTRACT

In view of the upcoming mega-constellations, Collision Avoidance Manoeuvres (CAM) become essential to protect both the space environment and the mission of the constellation. However, satellite constellations are usually bound to tight geometrical constraints, which can be disturbed by these manoeuvres. A communications Walker Delta constellation was analysed, using Inter-Satellite Laser Links (ISLL) to connect the satellites. For the encounters simulated, different CAM strategies were evaluated in terms of the evolution of the ISLL and the coverage. The results provide an insight into the impact of the manoeuvre parameters on the deviations from the nominal geometry and the coverage loss. Moreover, the impact of two simultaneous encounters was considered, as well as the fragmentation of a constellation satellite.

Keywords: mega-constellation; Collision Avoidance Manoeuvre; coverage; Inter-Satellite Laser Link.

1. INTRODUCTION

In the last few years, the launch of several satellite mega-constellations has been announced, which will place thousands of satellites in the already crowded Low Earth Orbit (LEO). Oneweb and Starlink have already started their deployment. Studies [6][5] analysed their impact on the space environment and proposed ways to mitigate it. In this context, Collision Avoidance Manoeuvres (CAMs) will not only help to protect the space environment, but also the mission of the constellation. A collision involving a constellation satellite can provoke a fragmentation cloud at the altitude of the constellation, entailing the need of more CAMs and threatening the survivability of the operational constellation satellites. Additionally, this could influence the performance of the constellation, forcing satellites to manoeuvre out of their nominal orbits and shortening their operational lifetime. Reference [8] shows the consequences of a collision cloud of constellation objects, revealing that the spatial density at the altitude range of the constellation would be dominated by the cloud.

The aim of this work is to analyse the impact of different manoeuvre strategies on the performance of the constellation. For the constellation defined, this impact will be examined on the evolution of the Inter-Satellite Laser Links (ISLLs), which are highly dependent on the geometry, and the coverage loss.

2. CASE STUDY

2.1. Constellation for the study

The case defined for the study intends to be as close as possible to the reality of the upcoming constellations while staying generic. The reason for this decision is twofold: firstly, it intends to avoid the loss of generality that implicitly comes with the choice of a specific constellation; secondly, it prevents the use of wrong assumptions in this study that could arise from a lack of information on existing constellations or changes in their design. Nonetheless, the purpose of this constellation will be assumed to be communications, since it is the purpose of the largest constellations that are currently being proposed. Consequently, the coverage was considered a driver of the constellation design, which is further explained in Section 2.2.1.

A $67° : 1080/24/12$ Walker Delta constellation at 600 km altitude was chosen for the study. The different parameters that define the constellation are explained below, as well as the reasons behind their choice:

- Walker Delta pattern: provides a symmetric pattern for a very uniform global coverage throughout all the latitudes L that verify $-(i + \lambda_{max}) < L < i + \lambda_{max}$, where i is the inclination of the orbits and λ_{max} the maximum Earth central angle (see Fig. 1).
- $h = 600km$: chosen to be as coherent as possible with the upcoming constellations. This altitude will result in a maximum Earth central angle of $\lambda_{max} = 15.8°$, assuming a grazing angle of $\varepsilon = 10°$.

- $i = 67°$: adequate to provide communication services to most populated areas around the world.
- $s = 45$: 45 satellites in each orbital plane, turning into a separation on the true anomaly θ of $\Delta\theta = 8°$ between satellites in the same orbital plane. This implies that there is a region of continuous coverage, or street of coverage, under each orbital plane. The width of this region or swath is $2\lambda_{street}$ with $\lambda_{street} = 15.3°$. More details can be found in [10].
- $p = 24$: 24 orbital planes, turning into a separation on the right ascension of the ascending node Ω of $\Delta\Omega = 15°$ between the orbital planes. Since $\Delta\Omega \approx \lambda_{street}$, the coverage from contiguous orbital planes will be superimposed, meaning that at least two satellites are seen at every moment from every point on Earth in the latitude range $-i < L < i$.
- $t = 1080$: total number of satellites, simply $s \cdot p$.
- $f = 12$: parameter defining the relative spacing between satellites in adjacent planes. $\Delta\phi$ is the phase difference between satellites in adjacent planes, which is calculated as $\Delta\phi = f \cdot 360°/t = 4°$. This phase difference maximizes the separation between the satellites when the orbits cross at the equator. Also, this implies that $\Delta\phi = \Delta\theta/2$; thus, the most susceptible zone to lose coverage is covered by the satellite in the adjacent orbit.

Regarding the physical characteristics of the spacecraft, a simple model with a cube of 1 m × 1 m × 1 m with two solar panels of surface 1 m × 3 m was used to calculate the average cross section using the CROC tool in ESA's software DRAMA. The resulting randomly tumbling cross section is 4.5910 m^2. This satellite has been assumed to weigh 200 kg, have a drag coefficient of 2.2 and a reflectivity coefficient of 1.1.

2.2. Parameters for the study

2.2.1. Coverage

The access area is defined as the total area on the ground that could potentially be seen at any moment by the satellite. The geometry determining the access area is shown in Fig. 1, where η represents the nadir angle, ε the grazing angle or spacecraft elevation angle, λ the Earth central angle and ρ the Earth angular radius.

The constellation was designed in such a way that at least two satellites can be seen at every moment from any point on Earth within the corresponding latitude range $-67° < L < 67°$. This was achieved by imposing a separation between planes at the equator that is approximately equal to the width of the street of coverage achieved by each plane [10]. The concept is shown in Fig. 2. This has been assumed to be a requirement for the constellation to provide the service, due to the high

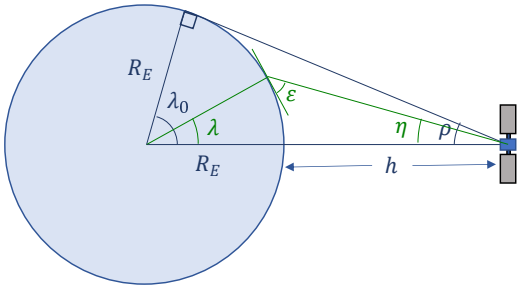

Figure 1. Geometry determining the access area

amount of traffic data expected. This configuration was also chosen for robustness on the fulfilment of the global coverage requirements: losing a satellite in this configuration would still not leave any point without coverage.

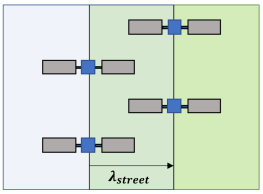

Figure 2. Design concept of the constellation to achieve the required coverage

2.2.2. Inter-Satellite Laser Link

Laser communication systems have many advantages over traditional radio frequency links, such as very high data transmission rate, no frequency license required, more secure due to the narrow divergence of the laser beam, a smaller size and lower power consumption [2], which makes them very suitable for large communication constellations.

But these links require highly precise pointing and synchronization. The high directionality of the laser beam implies that the optical axes of both terminals involved in the link must be accurately aligned [3], which could be a problem when a manoeuvre is performed.

The main requirements related to the Inter-Satellite Laser Link (ISLL) are therefore associated with the distance between the satellites; the beam pointing, defined by two angles: azimuth and elevation; and the slew rate, which is the rate of change of these angles with time [4]. These parameters are shown in Fig. 3.

The distance is easily calculated as the norm of the relative position vector between the satellites:

$$d = |\vec{r}_{rel}| = |\vec{r}_2 - \vec{r}_1| \tag{1}$$

From the sketch in Fig. 3, and considering the local horizon as the plane containing the in-track $\vec{t}$ and normal $\vec{n}$

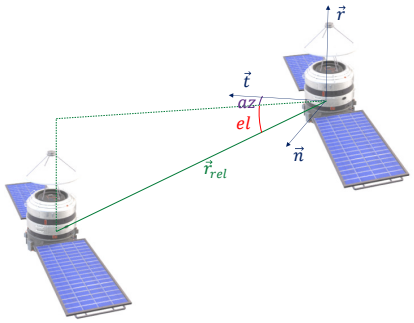

Figure 3. Geometry between the two satellites

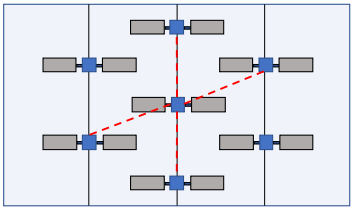

Figure 4. Configuration of the ISLL for one satellite.

vectors of the satellite reference frame, the azimuth az and elevation el angles are inferred:

$$el = \arcsin\left(\frac{\vec{r}_{rel} \cdot \vec{u}_r}{d}\right) \tag{2}$$

$$az = \arcsin\left(\frac{\vec{r}_{rel} \cdot \vec{u}_n}{d}\right) \tag{3}$$

Being $\vec{u}_r$ and $\vec{u}_n$ the unitary vectors in the radial and normal directions of the reference frame of the first satellite. The slew rate is defined as $d\,el/dt$ and $d\,az/dt$ for the elevation and azimuth respectively.

Four different links were assumed to be established by each satellite: two within the same orbital plane, and two with the adjacent orbital planes. This configuration is shown in Fig. 4.

2.3. Nominal Cases

The impact of the manoeuvre will be studied for four different situations:

- Case 1: One object crossing one orbital plane.
- Case 2: Two objects crossing the same orbital plane.
- Case 3: Two objects crossing two adjacent orbital planes.
- Case 4: Collision cloud in one of the constellation orbital planes.

Case 1 will be used to analyse the impact of a single manoeuvre on the constellation, and the effect that the choice of the different parameters and strategies has on this impact. Case 2 and Case 3 show the problems caused by two satellites manoeuvring at the same time. Finally, case 4 shows the issues that arise when a fragmentation occurs in one of the constellation planes.

3. MANOEUVRES

This study uses the simplest CAM strategies in order to be able to compare the impact of basic manoeuvre parameters. These manoeuvres aim to achieve a specific miss distance, either on the radial or the in-track direction. When aiming for a radial separation, the manoeuvres can be performed very close to the time of the encounter, but they require a bigger velocity change Δv. On the other hand, aiming for an in-track separation allows for more fuel-efficient manoeuvres, but requires an earlier execution of the manoeuvre. These manoeuvre strategies are further explained in Sections 3.1 and 3.2. The main source for these two sections is [9].

Once the encounter has been avoided, the satellite has to manoeuvre back to its nominal position. When the point at which the first manoeuvre was performed is reached again by the satellite after the encounter, thus when the satellite has been at the transit orbit for an integer number of revolutions, a new Δv is required to take the satellite back to its nominal orbit. Furthermore, due to the time spent in a different orbit with a different orbital period, the position of the satellite in the orbit will not be the same as before. Therefore, a new manoeuvre towards a new transit orbit and back is needed in order to re-adjust the phasing of the satellite (see Section 3.3). The different Δv that will be imposed to the satellite can be summarized as:

1. Δv_1: to move to the first transit orbit and avoid the collision.
2. Δv_2: to go back to the nominal orbit.
3. Δv_3: to move to the second transit orbit and re-adjust the phasing.
4. Δv_4: to go back to the nominal orbit and position.

It is important to note that Δv_2 and Δv_3 will normally be executed at the same time, but they have been separated for calculation purposes.

3.1. In-track separation: long-term strategies

This manoeuvre aims to achieve a specific in-track separation from the debris. To do so, the satellite will be

moved to a higher/lower orbit to modify its orbital period. As a consequence, it will arrive at the predicted encounter point later/earlier than the debris object involved in the conjunction, achieving the desired miss distance. The number of revolutions between the manoeuvre and the encounter will determine the separation achieved by a given transit orbit. The earlier the manoeuvre is performed, the smaller is the required variation of the semimajor axis, due to the longer time spent on the transit orbit. Fig. 5 shows a sketch of the manoeuvre.

If this manoeuvre is performed at the encounter point, n_{rev} revolutions before the encounter, the time at which it will get to the encounter point will change by $\Delta T \cdot n_{rev}$, being $\Delta T = T_{man} - T_{ref}$ the variation of the orbital period. The indices ref and man are used to identify the parameters on the reference orbit and the transit orbit after the manoeuvre, respectively, and enc is used for parameters at the encounter point before the manoeuvre is performed. Considering a constant orbital speed in the close region to the encounter, which is a good estimation for a circular/almost circular orbit, the in-track distance d achieved can be estimated as Eq. (4). This allows to calculate the required orbital period for the transit orbit T_{man} as shown in Eq. (5) and therefore the semimajor axis of the transit orbit a_{man} and the Δv_1 required for the CAM [9].

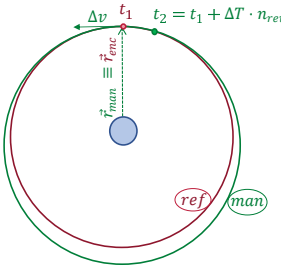

Figure 5. Sketch of the long term manoeuvre [9].

$$d \approx v_{ref} \cdot \Delta T \cdot n_{rev} \tag{4}$$

$$T_{man} = T_{ref} + \frac{d}{v_{ref} \cdot n_{rev}} \tag{5}$$

$$a_{man} = \sqrt[3]{\mu \left(\frac{T_{man}}{2\pi} \right)^2} \tag{6}$$

$$v_{man} = \sqrt{\mu \left(\frac{2}{r_{enc}} - \frac{1}{a_{man}} \right)} \tag{7}$$

$$\Delta v_1 = v_{man} - v_{ref} \tag{8}$$

3.2. Radial separation: short-term strategies

This manoeuvre aims to achieve a certain radial separation by directly increasing or decreasing the semimajor axis of the orbit. In order to maximize the radial reparation, it needs to be performed at the point of the orbit such that $\theta_{man} = \theta_{enc} \pm 180°$, being θ_{man} and θ_{enc} the true anomalies at the manoeuvre point and at the encounter point respectively. A sketch showing this type of manoeuvre can be found in Fig. 6. The calculation of the new radius at the encounter point r_{man}, the new semimajor axis a_{man}, and the required Δv_1 is shown in Eqs. (9)-(12) [9].

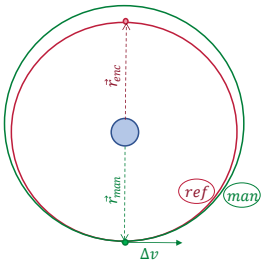

Figure 6. Sketch of the long term manoeuvre [9].

$$r_{man} = r_{ref} + d \tag{9}$$

$$a_{man} = a_{ref} + \frac{d}{2} = r_{ref} + \frac{d}{2} \tag{10}$$

$$v_{man} = \sqrt{\mu \cdot \left(\frac{2}{r_{ref}} - \frac{1}{a_{man}} \right)} \tag{11}$$

$$\Delta v_1 = v_{man} - v_{ref} \tag{12}$$

3.3. Re-phase manoeuvre

After the encounter, when $\theta = \theta_{man}$ is reached, Δv_2 is applied to return to the nominal orbit, which will have a similar magnitude and opposite direction to Δv_1. Since the satellite will have shifted from its nominal position, a new phasing manoeuvre needs to be performed. The new transit orbit will be lower than the nominal one if the first manoeuvre used a higher transit orbit, and vice versa. The satellite will stay in this second transit orbit for an integer number of revolutions, n_{ph}, before going back to its nominal orbit and position. Fig. 7 shows a sketch of a phasing manoeuvre using a lower transit orbit.

Let M_{ref} and M_{man} be the mean anomalies of the reference and the manoeuvred satellites respectively, so $\Delta M = M_{ref} - M_{man}$ is the phase change needed. The required orbital period of the new transit orbit is:

$$(2\pi \cdot n_{ph} - \Delta M) \cdot T_{ref} = 2\pi \cdot n_{ph} T_{ph} \tag{13}$$

$$T_{ph} = T_{ref} \cdot \left(1 - \frac{\Delta M}{2\pi n_{ph}} \right) \tag{14}$$

$$a_{ph} = \sqrt[3]{\mu \left(\frac{T_{ph}}{2\pi} \right)^2} \tag{15}$$

$$\Delta v_3 = \sqrt{\mu \cdot \left(\frac{2}{r} - \frac{1}{a_{ph}} \right)} - v_{ref} \tag{16}$$

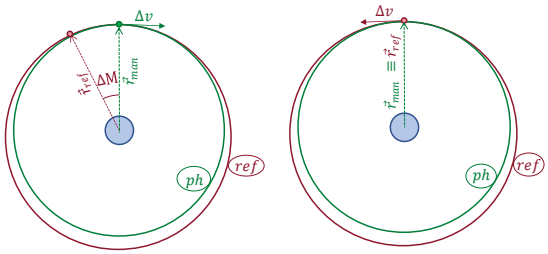

Figure 7. Phasing manoeuvre using a lower transit orbit.

After n_{ph} orbits, Δv_4 of similar magnitude and opposite direction to Δv_3, is used to take the satellite back to its nominal orbit and position.

4. METHODOLOGY

4.1. Creation of the encounters

To simulate realistic encounters, the Conjunction Data Messages (CDMs) provided by ESA for the Collision Avoidance Challenge were used [1] and modified to fit the constellation geometry. This provided a realistic evolution of the covariances with time.

4.1.1. Cases 1, 2 and 3

The process followed to modify the CDMs to simulate an encounter with a constellation satellite was as follows:

1. The constellation satellite that will undergo the encounter is defined.
2. An initial date is defined. The satellite is assumed to have the initial orbital parameters at this date, which will also be the date of creation of the first CDM.
3. From the initial date and the time to the time of closest approach (TCA) of the first CDM, the TCA date is inferred.
4. The constellation satellite is propagated to the TCA.
5. From the position of the constellation satellite at TCA and the relative positions of the encounter in the CDM, the position of the second object at TCA is calculated.
6. The CDMs are modified to include these characteristics, as well as the physical characteristics of both the constellation satellite and the debris object. The position of the debris object at TCA is updated in each CDM using the data of the new CDM. The creation date of each CDM is updated using the time difference between the CDMs and the start date.
7. These CDMs are used to calculate the collision probability of the encounter using the "maximum probability" method provided by OKAPI's endpoint. OKAPI:Orbits is a company providing Space Situational Awareness as a service, whose software was used for the development of this work [11].

This process was followed for all the events listed in the "train_data" file in [1] to eventually select a highly risky event for the study. The chosen event was ID 5726.

For cases 2 and 3 the same procedure is followed, but applied to two different constellation satellites. Therefore, two different objects and two different encounters are created. For simplicity, the same event (ID 5726) and start date were used for both satellites.

4.1.2. Case 4

The collision cloud was computed with OKAPI's implementation of NASA's Standard Breakup model of Evolve 4.0 [7]. The resulting file with the orbital parameters and the physical characteristics of the fragments was then used as an input for OKAPI's SSA platform to find encounters closer than 1 km in all the radial, in-track and normal directions.

To create the CDMs and calculate the collision probability, the covariances from the event 5726 of the [1] database were used, selecting the ones corresponding to the most similar *time to TCA*, assuming for simplicity that the CDMs were created at the time of the fragmentation.

4.2. Procedure

Firstly, the next parameters are defined for the CAM:

a) The desired miss distance.

b) The direction in which this distance should be achieved ('r' for radial and 't' for in-track).

c) The time at which the manoeuvre will be performed, expressed as $\Delta t_{m-tca} = t_{tca} - t_{man}$.

d) The number of orbits in which the phase will be adjusted n_{ph}.

Secondly, the process is as follows:

1. The initial conditions are defined and the CDMs are created following the process in 4.1.
2. From the TCA and the $\Delta t_{m-tca} = t_{tca} - t_{man}$, the date and time of the manoeuvre is inferred.
3. The propagation starts form the initial date, which is also the date of creation of the first CDM. When each CDM is received, the risk is checked.

4. When the time of the manoeuvre is reached, the manoeuvre is performed if the risk of the last CDM was higher than a predefined threshold, set to 10^{-4}.

5. If the manoeuvre type chosen was in-track, Δv_1 is calculated and added. If the manoeuvre type was set to radial, the satellite is propagated until it forms 180° with the expected encounter point. Subsequently, Δv_1 is calculated and added. From now on, two satellites will be propagated at the same time: one reference satellite which will stay in the nominal orbit, and the manoeuvred satellite.

6. The satellites are propagated until the TCA is reached. During this time, the risk is recalculated for each CDM with the new expected position of the satellite at TCA, making sure that it stays below the threshold.

7. The satellites are propagated until they reach the point where the first manoeuvre was performed. Then, the reference satellite is used to calculate the velocity that the manoeuvred satellite should have in order to be in the nominal orbit. Δv_2 is therefore calculated and added.

8. The Δv_3 required to adjust the phasing in n_{ph} orbits is calculated and added. Eqs. (14)-(16) are used. To gain accuracy, ΔM is calculated as the angle between the position vectors of both satellites, $\vec{r}_{man}$ and $\vec{r}_{ref}$, thus : $\Delta M = \arccos \frac{\vec{r}_{man} \cdot \vec{r}_{ref}}{|\vec{r}_{man}| \cdot |\vec{r}_{ref}|}$.

9. The satellites are propagated for n_{ph} orbits.

10. The reference satellite is used to calculate the Δv_4 needed, and the manoeuvred satellite comes back to its nominal orbit and position.

Even if this process refers only to the satellite undergoing the encounter, the satellites connected to this one by ISLLs are propagated at the same time, in order to be able to compute the evolution of the geometry.

When several encounters take place, the process remains the same, with the only complication of considering the CDMs, TCAs and manoeuvres corresponding to the different events in the same timeline.

The coverage loss or visibility loss was defined as the area that should be seen from the satellite when no manoeuvre is performed, but is not seen anymore after the manoeuvre. therefore, it was evaluated at each time step as:

$$V_{loss} = \frac{A_{loss}}{A_{ref}} \cdot 100\% = \frac{A_{ref} - A_{int}}{A_{ref}} \cdot 100\% \quad (17)$$

Where A_{ref} is the access area of the reference satellite, thus the area that would be seen from the satellite if no manoeuvre was performed; A_{loss} is the area that should be seen from the satellite but it is not seen once the manoeuvre is performed; A_{int} is the intersection between the access areas of the reference and the manoeuvred satellite; and V_{loss} is the percentage of the reference access area that is not seen anymore. These areas were calculated assuming planar geometry, which might affect the accuracy of the results.

In order to asses the evolution of the ISLL, the azimuth, elevation and distance and slew rates were computed at each time step. For the first three parameters, Eqs. (1)-(3) were used. The slew rates were estimated as:

$$\left(\frac{d\,el}{dt}\right)_i = \frac{el_{i+1} - el_{i-1}}{2\Delta t} \quad \left(\frac{d\,az}{dt}\right)_i = \frac{az_{i+1} - az_{i-1}}{2\Delta t} \quad (18)$$

Where Δt is the magnitude of the time step and the index i represents each time step.

4.3. Setup of the simulations

Due to the influence of orbital perturbations, the orbital elements of the satellites keep varying over time. When the orbit is defined, the mean orbital elements are usually considered, but in reality the position of the satellite at each time corresponds to its osculating orbital elements. The propagator used for the simulations was Neptune, provided by OKAPI's API and accessed with the Python connector. A first study with only two satellites has been performed considering the most important perturbations, thus geopotential up to 6th degree, atmospheric drag, third body perturbations from the Sun and the Moon, solar radiation pressure and solid tides. After, the simulations for more satellites have been carried out without perturbations.

5. CASE 1: ONE OBJECT CROSSING ONE ORBITAL PLANE

5.1. Encounter description

The first case that will be discussed consists of one object crossing one orbital plane. The initial mean orbital elements of the satellites considered are shown in Tab. 1. Sat1 is assumed to undergo the encounter. The study is first carried out only for Sat1 and Sat2 considering perturbations. Then, the variations with respect to the other satellites are examined, without considering perturbations.

	Sat1	Sat2	Sat3	Sat4	Sat5
$a\,(km)$	6978	6978	6978	6978	6978
e	0	0	0	0	0
$i\,(°)$	67	67	67	67	67
$\Omega\,(°)$	0	0	0	15	15
$\omega\,(°)$	0	0	0	0	0
$M\,(°)$	0	8	-8	4	-4

Table 1. Mean orbital elements of the satellites.

In the case with only two satellites, the C-state tool of ESA's DRAMA software has been used to transform the orbital elements of the Sat1 from mean to osculating. Then, this satellite was propagated for the time needed to cover 8° in mean anomaly, thus for $8 \cdot T_{mean}/360$, in order to obtain the initial conditions for the Sat2. This approach lacks some accuracy, but more complex methods to improve the accuracy of these orbital elements are out of the scope of this work and are not expected to affect the usefulness of the results. This is not necessary when analysing the 5 satellites, since no perturbations were considered.

Finally, the data from the event 5726 in [1] was used to create the encounter, following the process in Section 4.1.

The relative position of the object with respect to Sat1 is positive in both radial and in-track directions. This implies that the radial manoeuvre is performed towards a lower orbit in order to achieve a larger miss distance, while the in-track manoeuvre uses a higher orbit to delay the arrival to the encounter point.

The parameters that will be varied and whose impact will be studied are the desired miss distance, the direction in which it should be achieved (radial or in-track), the time between the manoeuvre and the expected TCA (Δt_{m-tca}), and the number of revolutions that the satellite will stay in the phasing transit orbit (n_{ph}). The results will be presented as follows: first, the collision probability, the visibility loss and the Δv requirements are studied for different values of the miss distance for both the radial and in-track cases, aiming to determine a reasonable value for the miss distance. Afterwards, this value will be used for the simulations that will show the variations in the coverage and the geometry of the inter-satellite link depending on the values of Δt_{m-tca} and n_{ph}.

5.2. Intended Miss Distance

Figs. 8 - 13 show that, as expected, the collision probability decreases more for a larger miss distance. However, to reach higher values of the miss distance, a bigger Δv is required. Additionally, a bigger orbit change also causes a bigger visibility loss. When comparing in-track and radial manoeuvres, the reduction of the collision probability is higher for the radial manoeuvre, but the fuel consumption and the visibility loss are higher as well. Thus, the optimum value is the one that provides a low enough collision probability without compromising the coverage or significantly increasing the fuel consumption. As a trade-off, $d = 1$ km is used for the in-track manoeuvres and $d = 0.2$ km for the radial manoeuvres in this work.

5.3. Inter-satellite Link

First, the geometry of the ISLLs has been examined without any manoeuvre. When no perturbations are considered, the geometry between satellites in the same plane

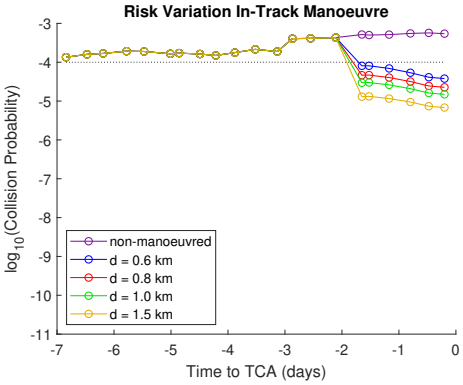

Figure 8. Risk variation for the in-track manoeuvre for various miss distances with $\Delta t_{m-tca} = 2$ and $n_{ph} = 14$. Every point represents a CDM received.

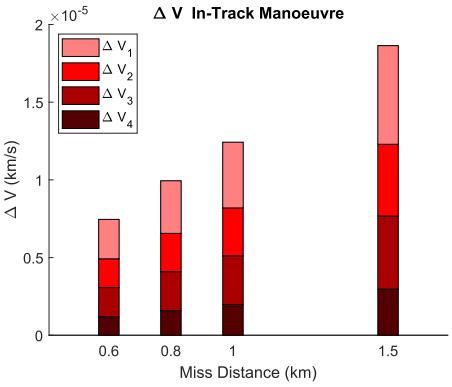

Figure 9. ΔV required for the in-track manoeuvre for various miss distances with $\Delta t_{m-tca} = 2$ and $n_{ph} = 14$.

remains constant, with $d \approx 973.5$ km, $el = -4°$, and $az = 0°$ for the Sat2 and $az = 180°$ for Sat3. Conversely, the geometry between satellites in adjacent planes varies throughout the orbit, with minimum distance and elevation next to the poles. Tab. 2 summarizes the minimum requirements for the laser terminal inferred from the geometry without manoeuvre. This is only intended to provide a reference of the variations in the geometry on nominal conditions, in order to understand which further variations caused by the manoeuvre could be problematic, but it does not correspond with any existing laser terminal.

To understand better the geometry between the satellites, Figs. 14-15 show the elevation versus the azimuth of Sats 2 to 4 from Sat1 throughout one orbit.

Next, the variations in the ISLL depending on the manoeuvre parameters are discussed. The geometry between Sat1 and Sat2 considering perturbations is shown and discussed first, followed by a comparison of the evolution of the ISLL for all satellites. The plots in this section only show the differences in the geometry between the manoeuvred and the non-manoeuvred cases, thus $\Delta d = d_{man} - d_{ref}$, $\Delta el = el_{man} - el_{ref}$ and

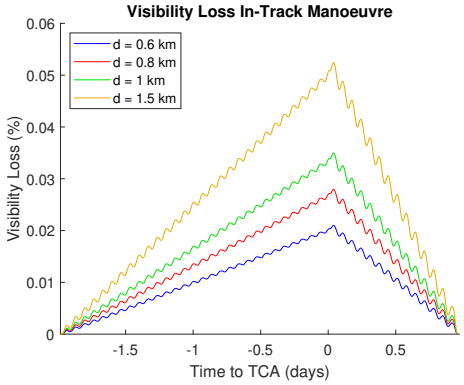

Figure 10. Visibility loss for the in-track manoeuvre for various miss distances with $\Delta t_{m-tca} = 2$ and $n_{ph} = 14$.

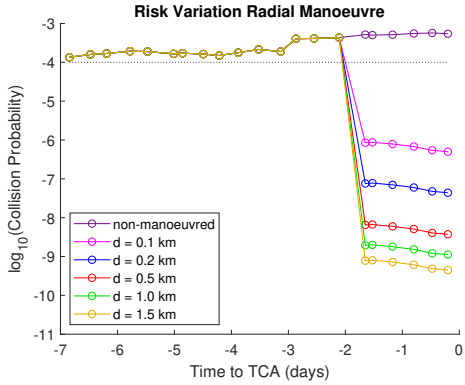

Figure 11. Risk variation for the radial manoeuvre for various miss distances with $\Delta t_{m-tca} = 2$ and $n_{ph} = 14$. Every point represents a CDM received.

$\Delta az = az_{man} - az_{ref}$.

Parameter	Nominal range
Distance	$970km < d < 2060km$
Elevation	$-9° < el < -4°$
Azimuth	$-55° < az < 55°$
Slew Rate Elevation	$< 0.005°/s$
Slew Rate Azimuth	$< 0.1°/s$

Table 2. Laser terminal requirements for the constellation derived from the simulations.

5.3.1. In-Track versus Radial Manoeuvre

Due to the geometry of the encounter these manoeuvres are performed in opposite directions: the radial manoeuvre uses a lower transit orbit, while the in-track manoeuvre uses a higher one. Therefore, the variations in the geometry between the satellites will evolve in opposite directions. Moreover, the magnitude of the radial manoeuvre is bigger than the magnitude of the in-track manoeuvre. Therefore, the deviations from the nominal geometry are bigger for this case. This is shown in Figs.16-20.

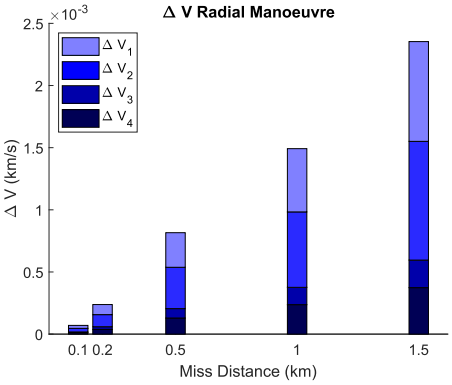

Figure 12. ΔV required for the radial manoeuvre for various miss distances with $\Delta t_{m-tca} = 2$ and $n_{ph} = 14$.

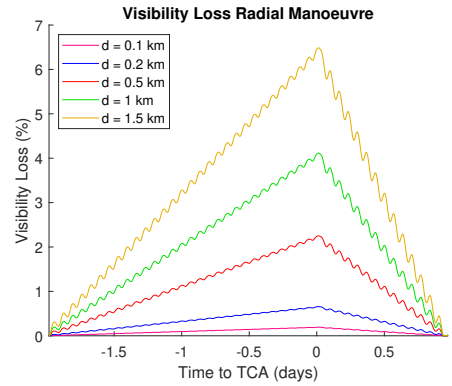

Figure 13. Visibility loss for the radial manoeuvre for various miss distances with $\Delta t_{m-tca} = 2$ and $n_{ph} = 14$.

When Sat1 moves to a lower orbit (radial manoeuvre) the smaller orbital period makes it drift towards Sat2. Therefore, the distance decreases and Sat2 gets closer to the line of sight of Sat1, causing positive deviations in the elevation. When Sat1 moves to a higher orbit (in-track manoeuvre), its orbital period increases so it drifts backwards, further from Sat2. Thus, the distance increases and the elevation decreases. On the other hand, the satellite remains within the same orbital plane, so the variations in the azimuth are very small and oscillate around 0. The deviations in the slew rate are small and oscillate around 0, with increasing amplitude for the azimuth and constant for the elevation. In the elevation they will be

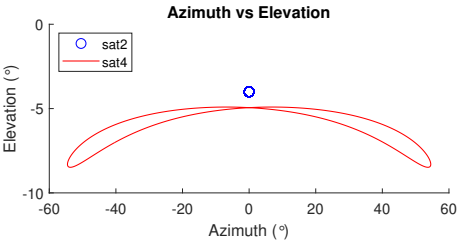

Figure 14. Azimuth an elevation of Sat2 and Sat4.

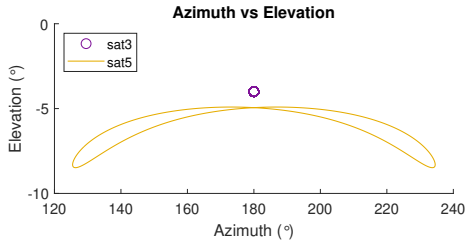

Figure 15. Azimuth an elevation of Sat3 and Sat5.

dominated by the last phasing orbits, which require the biggest orbital change. This

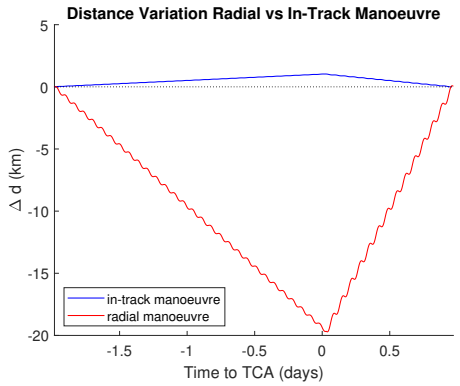

Figure 16. Distance variation for the in-track and radial manoeuvres with $\Delta t_{m-tca} = 2$ and $n_{ph} = 14$.

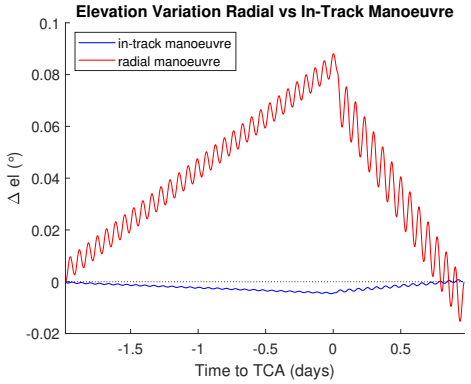

Figure 17. Elevation variation for the in-track and radial manoeuvres with $\Delta t_{m-tca} = 2$ and $n_{ph} = 14$.

5.3.2. Time of the manoeuvre before TCA

Due to the differences on how the manoeuvres are calculated, the impact of the Δt_{m-tca} is different for the in-track and radial strategies. The orbital change needed for the in-track manoeuvre is bigger the later the manoeuvre is performed, turning into a steeper growth of the deviations for later manoeuvres. As a consequence, the magnitude of the deviations at TCA is nearly the same for all values of Δt_{m-tca}. On the other hand, the transit orbit

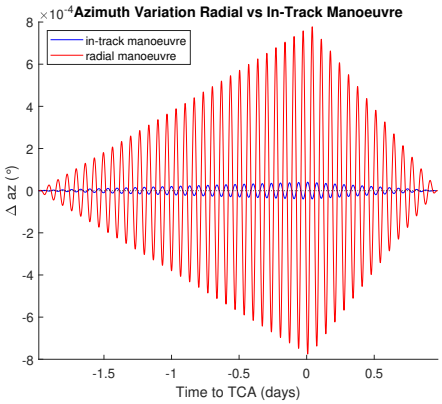

Figure 18. Azimuth variation for the in-track and radial manoeuvres with $\Delta t_{m-tca} = 2$ and $n_{ph} = 14$.

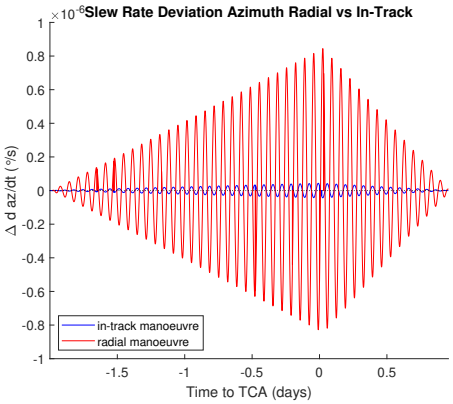

Figure 19. Deviation of the slew rate of the azimuth for both in-track and radial manoeuvres with $\Delta t_{m-tca} = 2$ and $n_{ph} = 14$.

used for the radial manoeuvre is always the same, regardless of the time of execution of the manoeuvre. Thus, the variations in the geometry will always increase with time at the same pace, leading to much bigger deviations for the earlier manoeuvres (Figs. 21-24).

5.3.3. Number of revolutions in the phasing orbit

Smaller values of n_{ph} imply a faster re-phasing, but also require a bigger Δv. For the results shown here (Figs. 21-24), the values of n_{ph} are not problematic for the distance nor the elevation between satellites. However, it was observed that when very small values of n_{ph} are used they can provoke peaks on the elevation and its slew rate that are bigger that those caused by the CAM itself. These results were considered to be too far from the operational case to be shown here, but it is important to keep in mind that both the CAM and the phasing manoeuvre must be equally planned.

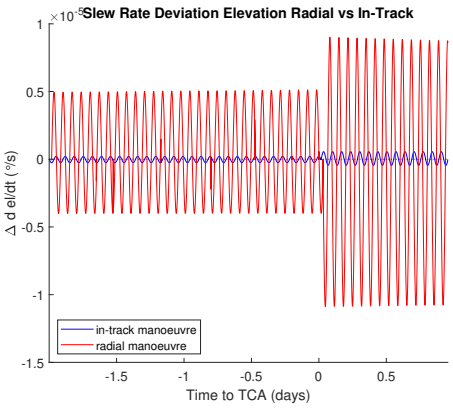

Figure 20. Deviation of the slew rate of the elevation for both in-track and radial manoeuvres with $\Delta t_{m-tca} = 2$ and $n_{ph} = 14$.

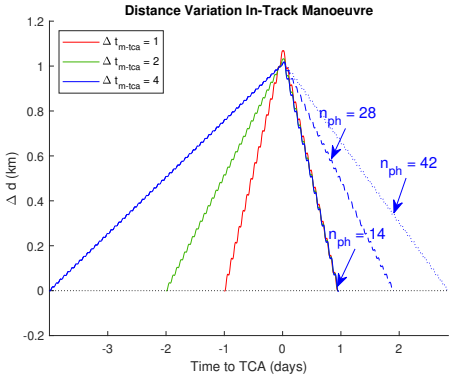

Figure 21. Distance variation for the in-track manoeuvre for different values of Δt_{m-tca} and n_{ph}.

5.3.4. 5 satellites

Turning perturbations off, the geometry between Sat1 and the rest of satellites in Tab. 1 has been examined. The deviations in the geometry with respect to the satellites that are positioned ahead Sat1 (Sat2 and Sat4) vary in the opposite direction to those that are positioned behind (Sat3 and Sat5). On the other hand, the oscillations are always bigger for the inter-plane links (Sat4 and Sat5). The elevation always evolves oppositely to the distance: when the satellites get closer, the elevation increases to get closer to the line of sight at 0°. The magnitude of the deviation in the distance reaches approximately the same maximum values for all the satellites. The biggest deviations were found, unsurprisingly, for the radial manoeuvre with $\Delta t_{m-tca} = 4$ and $n_{ph} = 14$. These deviations correspond to a maximum variation in the distance of around 30 km, and around 0.14° in the elevation. The deviations in the azimuth are dominated by the inter-plane links, reaching values of almost 0.8°. On the other hand, the requirements in slew rate will be dominated by the requirements in azimuth for the inter-plane links, but the deviations are small in comparison with the require-

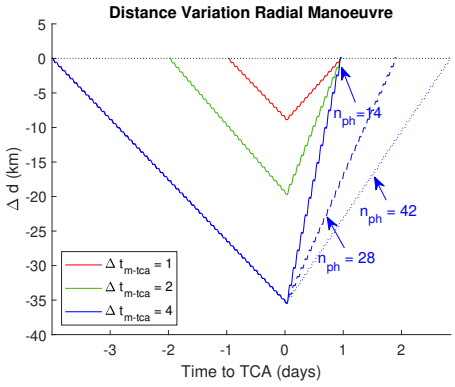

Figure 22. Distance variation for the radial manoeuvre for different values of Δt_{m-tca} and n_{ph}.

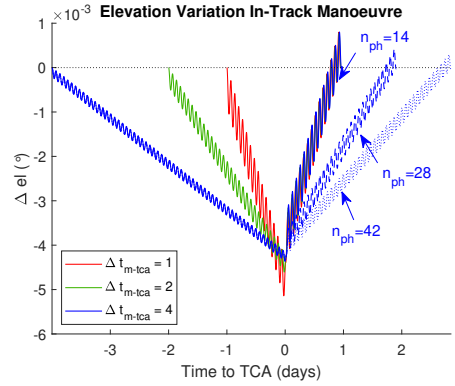

Figure 23. Elevation variation for the in-track manoeuvre for different values of Δt_{m-tca} and n_{ph}.

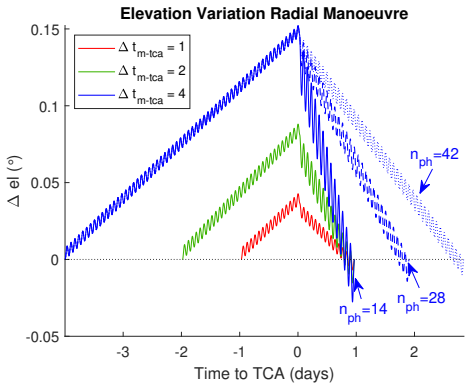

Figure 24. Elevation variation for the radial manoeuvre for different values of Δt_{m-tca} and n_{ph}.

ments stated for the case without manoeuvre (Tab. 2), reaching values about 0.002°, while they are of the order of $6 \cdot 10^{-5}$ ° for the elevation. However, the importance of using reasonable values of n_{ph} is demonstrated again, since the same CAM using $n_{ph} = 4$ for the phasing manoeuvre would provoke deviations of about 0.2° on the elevation, and up to 0.44° when $n_{ph} = 1$ is used.

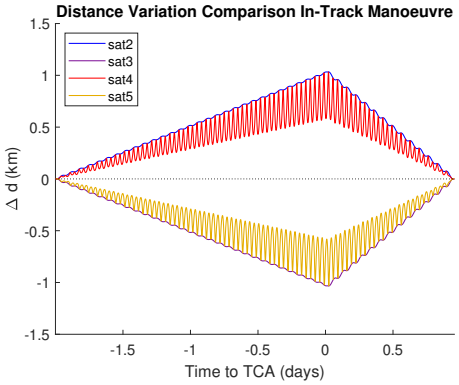

Figure 25. Distance variation for the radial manoeuvre with respect to different satellites with $\Delta t_{m-tca} = 2$ and $n_{ph} = 14$.

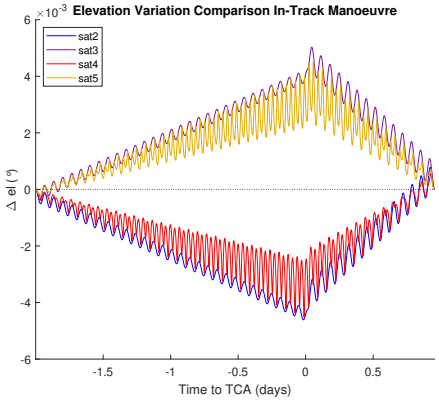

Figure 26. Elevation variation for the radial manoeuvre with respect to different satellites with $\Delta t_{m-tca} = 2$ and $n_{ph} = 14$.

5.4. Coverage

The variations in the coverage are consequence of two aspects: the deviation of the ground-track and the variation of the λ_{max}, thus the size of the region that can be observed from the satellite. While the deviation of the ground-track will always have a negative impact on the visibility, the variation of the λ_{max} can be beneficial when a higher transit orbit is being used, since a larger access area can compensate to some extent the deviation of the subsatellite point.

The visibility loss has been computed as in Eq. (17). The visibility loss is remarkably larger for the radial manoeuvre, rather than the in-track one. This is a consequence of both a bigger deviation of the ground-track and the fact that in this case a lower orbit is used, due to the geometry of the encounter, turning into a smaller access area. For the radial manoeuvre, the earlier the manoeuvre is performed the larger visibility loss is. On the other hand, the differences between transit orbits depending on the time of execution for the in-track manoeuvres turn into a very similar maximum visibility loss for all cases.

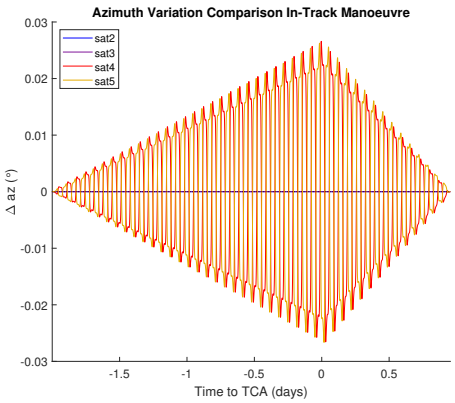

Figure 27. Azimuth variation for the radial manoeuvre with respect to different satellites with $\Delta t_{m-tca} = 2$ and $n_{ph} = 14$.

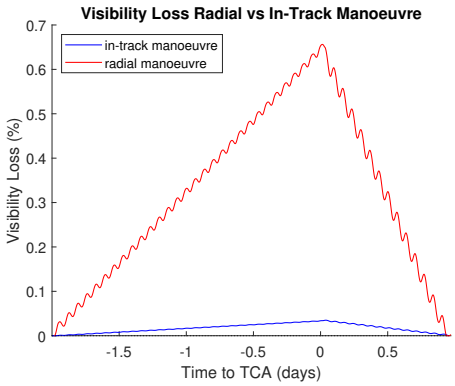

Figure 28. Visibility loss for the in-track and the radial manoeuvres, with $\Delta t_{m-tca} = 2$ days and $n_{ph} = 14$

5.5. DeltaV

Even if the optimization of the Δv required is out of the scope of this work, it provides very useful information about the magnitude of the orbital change performed and the operational impact of the manoeuvre. First, the radial manoeuvre requires a much higher Δv than the in-track manoeuvre. This difference is even bigger for higher Δt_{m-tca}. This is due to a reduction of the fuel needed for the in-track manoeuvre and an increase of the fuel needed for the re-phasing manoeuvre after a longer stay in the transit orbit.

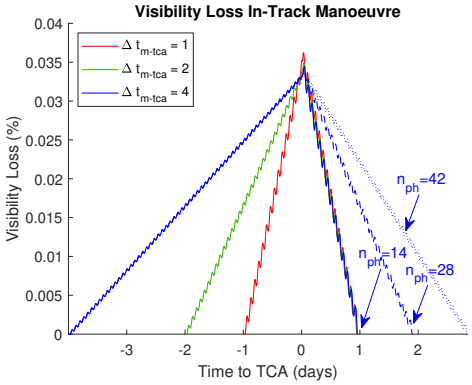

Figure 29. Visibility loss for the in-track manoeuvre for different Δt_{m-tca} and n_{ph}

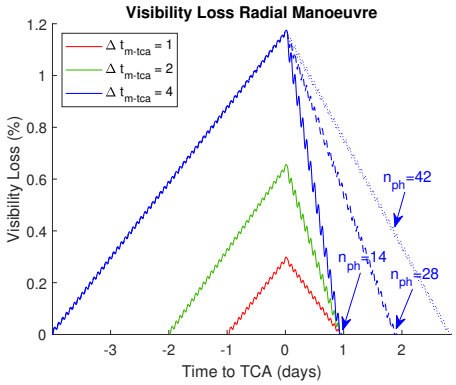

Figure 30. Visibility loss for the radial separation case for different Δt_{m-tca} and n_{ph}

Figs. 31 shows the Δv required when $n_{ph} = 14$ for different values of Δt_{m-tca}, distinguishing between the amount spent in each impulse. The different Δv were explained in Section 3. For the radial manoeuvre, the first transit orbit is the same for all values of Δt_{m-tca}, so Δv_1 and Δv_2 remain unchanged. However, more time spent on the first transit orbit implies a bigger manoeuvre needed for re-phasing, so Δv_3 and Δv_4 increase with Δt_{m-tca}. Conversely, the in-track manoeuvres always reach a similar phase shift, so the magnitude of Δv_3 and Δv_4 are similar for all values of Δt_{m-tca}, while earlier manoeuvres help to reduce Δv_1 and Δv_2. On the other hand, Fig. 32 shows that higher values of n_{ph} always help to reduce the Δv needed for the phasing manoeuvre.

6. CASE 2: TWO OBJECTS CROSSING THE SAME ORBITAL PLANE

In order to examine the maximum impact on the variations of the ISLL, two contiguous satellites were chosen to undergo the encounters, Sat1 and Sat2 in Tab. 1. For simplicity, the same event (5726) and start date was used for the encounters with both satellites. For these two satellites, perturbations are considered in the propagation.

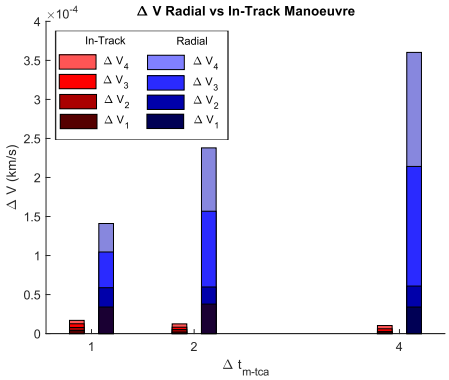

Figure 31. Δv required for the in-track and radial manoeuvres for different Δt_{m-tca} with $n_{ph} = 14$.

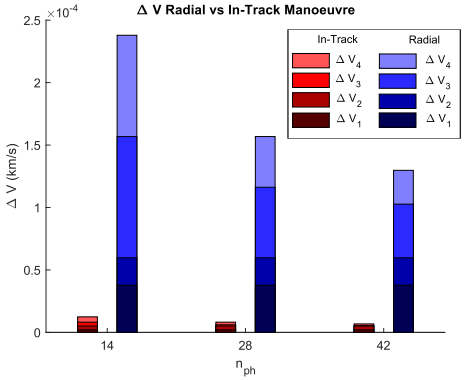

Figure 32. Δv required for the in-track and radial manoeuvres for different n_{ph} with $\Delta t_{m-tca} = 2$.

Again, due to the geometry of the encounter, the radial manoeuvre uses a lower transit orbit, while the in-track manoeuvre uses a higher one. Different combinations of these types of manoeuvres have been used in the simulations. An overview of the effects is shown below, supported by Figs. 33-34:

- Sat1 in-track + Sat2 in-track: both satellites move to a similar higher orbit, so the impact of the manoeuvre on the geometry between them is very small.
- Sat1 in-track + Sat2 radial: Sat1 moves to a higher orbit, thus drifting backwards, and Sat2 to a lower orbit, thus drifting forward. The two effects add up and both satellites drift apart faster than in Case 1.
- Sat1 radial + Sat2 radial: both satellites move to a similar lower orbit, so the impact of the manoeuvre on the geometry between them is very small.
- Sat1 in-track + Sat2 radial: Sat1 moves to a lower orbit, thus drifting forward, and Sat2 to a higher orbit, thus drifting backwards. The two effects add up and both satellites drift closer faster than in Case1.

Since the magnitude of the deviations is much bigger for the radial manoeuvre than for the in-track manoeuvre, the

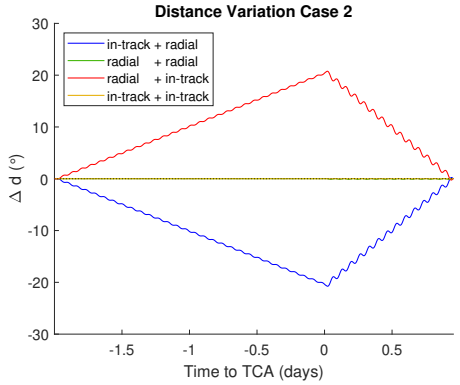

Figure 33. Distance variation with different combinations of manoeuvres for Sat1 and Sat2, $\Delta t_{m-tca} = 2$ and $n_{ph} = 14$.

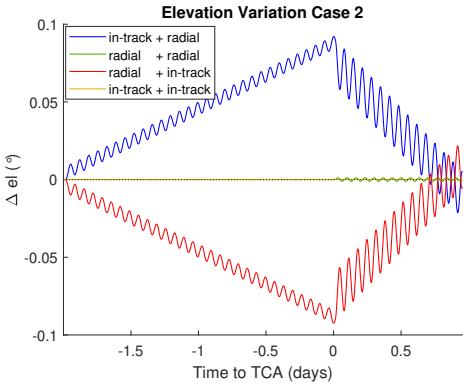

Figure 34. Elevation variation with different combinations of manoeuvres for Sat1 and Sat2, $\Delta t_{m-tca} = 2$ and $n_{ph} = 14$.

effects caused by this manoeuvre dominate the results. Hence, the higher deviations found for this case do not differ significantly from the deviations found for the radial manoeuvre in Case 1. However, situations in which both satellites need to perform a radial manoeuvre in opposite directions should be further studied.

7. CASE 3: TWO OBJECTS CROSSING ADJACENT ORBITAL PLANES

To analyse the maximum impact on the variations of the ISLL, two contiguous satellites have been chosen to undergo the encounters, Sat1 and Sat4 in Tab. 1. Again, the same event (5726) and initial date were used to generate the encounters with both satellites. Perturbations are not considered for any propagation in this section, since they were not used either for the evaluation of the ISLL between these satellites in the previous sections.

As in Case 2, different combinations of radial and in-track manoeuvres were simulated, providing very similar results as in Section 6: when the manoeuvres are performed in the same direction, the effects compensate each other and the variations on the geometry are small; conversely, when the manoeuvres are executed in opposite directions, the effects add up and the deviations are bigger than in Case 1.

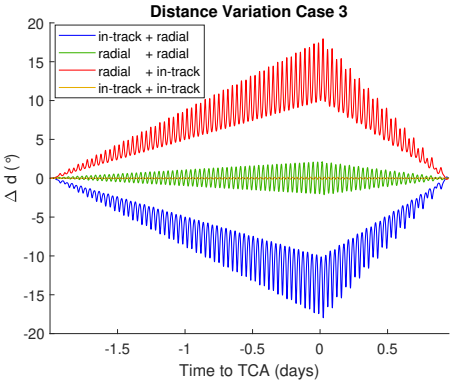

Figure 35. Distance variation with different combinations of manoeuvres for Sat1 and Sat4, $\Delta t_{m-tca} = 2$ and $n_{ph} = 14$.

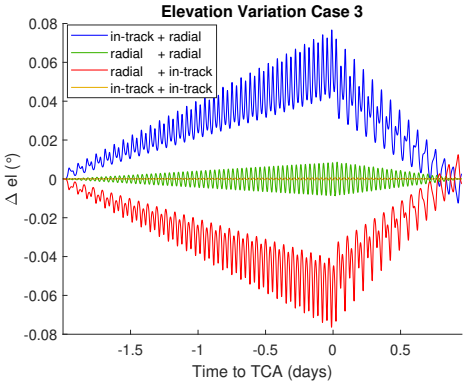

Figure 36. Elevation variation with different combinations of manoeuvres for Sat1 and Sat4, $\Delta t_{m-tca} = 2$ and $n_{ph} = 14$.

It is interesting to note that, while the variations for the "in-track + radial" or "radial + in-track" cases show a steady growth or decrease that would lead to big deviations in the long term if the orbit is not corrected, the variations when both manoeuvres are in-track or radial oscillate around zero. Thus, the mean geometry within these satellites would roughly remain unchanged, even if they stayed in the transit orbits for a longer period of time. This is due to the fact that both manoeuvres are approximately the same, and were performed at the same time, since the same CDM data was used to create the encounters. Therefore, the transit orbits of both satellites are nearly equal and they keep orbiting in formation flight (only between the two of them).

8. CASE 4: COLLISION CLOUD

As explained in Section 4.1.2, a fragmentation was assumed to occur for a constellation satellite. 217 encounters closer than 1 km have been found over a period of one week. The covariances from the event 5726 were used to build the CDMs, always using the value of the CDM with the most similar *time to TCA*, and calculate the risk of each encounter. Five encounters with a risk higher than 10^{-5} were found. At the defined initial date, all satellites were placed at their initial positions and the fragmentation was simulated for the chosen satellite. Then, manoeuvres were performed as follows:

- If the time between the start date and the TCA is smaller than 1 day, a radial manoeuvre is performed just half an orbit before the encounter.
- If the time between the start date and the TCA is smaller than 2 days but bigger than 1, an in-track manoeuvre is performed 1 day before TCA.
- If the time between the start date and the TCA is bigger than 2 days an in-track manoeuvre is performed 2 days before TCA.

Consequently, one radial manoeuvre and four in-track manoeuvres 2 days before TCA were performed. However, the time needed to realise that there has been a fragmentation, track the pieces and plan the manoeuvre is not taken into account in this approach, and in practise it would probably not be possible to perform the manoeuvres that soon. These risky encounters did not occur for contiguous satellites, thus they did not resemble Cases 2 or 3 which cause the most problematic situations. Nevertheless, the approximation used for the covariances lacks accuracy, so it is worth to look at all the close encounters found. To do so, it is necessary to look at the initial position of the satellites that undergo the encounters and at the date of these encounters, as shown in Fig. 37.

It can be seen that there are many encounters occurring between satellites connected by an ISLL, thus satellites that are in the same or adjacent planes in contiguous positions in mean anomaly. If these encounters occur at close times, the situations described in Sections 6 and 7 can arise. The clusters observed in 37 suggest that many problematic encounters might arise, so a further analysis has been carried out.

Considering the characteristics of the constellation and the way the ISLL was defined, the encounters were filtered to find, for each of them, any other encounter that occurs at a time difference of maximum 3 days at position that is linked to that satellite. Finally, 127 constellation satellites have been found to be involved in 119 problematic encounters, 58 of which occurred within the same orbital plane (Case 2) and 61 within adjacent planes (Case 3).

The limit of 3 days difference in the TCA of the encounters was considered a reasonable approach of the time that

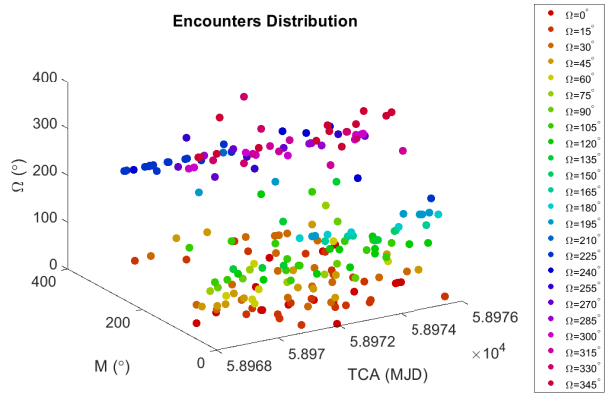

Figure 37. Initial right ascension of the ascending node Ω and mean anomaly M of the satellites involved in the encounters and TCA of these encounters expressed in Modified Julian Date (MJD). The encounters are color-coded for Ω to help visualization.

a satellite would stay in a different orbit, taking into account both the avoidance and the re-phasing manoeuvres. However, if a fragmentation has taken place at the constellation altitude, different strategies for the manoeuvres should be considered. By reducing the time limit to one day out of the nominal orbit, the number of problematic encounters is reduced to 37. This suggests that, in some situations, smaller times out of the nominal orbit should be prioritized. Therefore, when a fragmentation has occurred and several manoeuvres have to be performed, the expected encounters of all the satellites should be taken into account when the collision avoidance manoeuvre is designed in order to reduce the impact on the constellation geometry. Additionally, the probability of causing a new encounter with other fragments when a manoeuvre is performed will probably be high, imposing many limitations on the CAMs to be performed.

Moreover, the encounters shown here were founded over a period of just one week. When so many encounters are expected to occur due to the fragments orbiting at the altitude of the constellation, an operator might consider to raise all the satellites of the constellation for some time in order to avoid these encounters and maintain the geometry of the constellation.

9. CONCLUSION

The impact of the collision avoidance manoeuvres on large satellite constellations has been studied with regard to the coverage and the geometry of the constellation, which influences the ISLL. Different strategies and combinations of parameters have been varied in order to analyse their effect on this impact.

These results have many limitations, mainly coming from the very simple strategies considered for the manoeuvres and the absence of operational considerations on the planning on these manoeuvres. Additionally, the accuracy of

the results was affected by not considering the perturbations on the propagations with more than two satellites and by the simple approach used to convert from mean to osculating orbital elements. However, this is not expected to affect the usefulness of the results.

Strategies aiming for an in-track separation have demonstrated to be more efficient than radial manoeuvres, reducing the impact of the manoeuvre in both the geometry and the loss of coverage and requiring of a smaller Δv and therefore less propellant for their execution. On the other hand, strategies aiming a radial separation are recommended when a large reduction of the collision probability is needed in a short time. Generally, the manoeuvre strategy chosen will be a trade-off between the Δv used for the manoeuvre and the time spent on a different orbit.

However, in real life manoeuvre planning other operational constraints might apply, like coordination with station keeping manoeuvres or other catalog objects that could could create new encounters, limiting the possible manoeuvre strategies. Also, the rest of catalogued objects need to be taken into account when any manoeuvre is planned, in order to prevent creating an even more risky encounter with a different object.

The manoeuvre used to readjust the phasing after the encounter has demonstrated to deserve attention as well: when a small number of revolutions in this transit orbit is used, it can cause the greatest deviations in some parameters and the biggest fuel expense. Larger values of n_{ph} diminish the orbit change required for the phasing, reducing the fuel used and the deviations from the nominal parameters.

The results obtained demonstrate the importance of a good manoeuvre design, showing the impact that a wrong choice of the manoeuvre parameters can have in terms of both Δv and performance of the constellation. They also show the importance of considering these manoeuvres from the design stage of the constellation, in order to include enough flexibility on the geometry requirements of the constellation so that they will not be disturbed by these manoeuvres. These geometry requirements will be determined by both the requirements of the laser terminal and the layout of the constellation, in addition to the mission of the constellation.

Moreover, a lot of work remains to be done: optimized strategies for the manoeuvres need to be considered, as well as the use of electric propulsion and their coordination with the station keeping of the spacecraft and other operational constraints or the rest of catalog objects. Better strategies should be defined to face situations like the collision cloud. Further analysis to see which parts of the area missed by the manoeuvred satellite are still covered by the other satellites would also be needed.

ACKNOWLEDGEMENTS

The work leading to this publication was performed by Lucía Ayala Fernández as Master Thesis at OKAPI:Orbits as part of her Joint Master Program in Space Science and Technology – SpaceMaster at Luleå University of Technology and Université Toulouse III - Paul Sabatier. OKAPI:Orbits is a company, providing Space Situational Awareness as a service, with focus on constellation operators. More information can be found at [11].

REFERENCES

1. Collision Avoidance Challenge: Data, *https://kelvins.esa.int/collision-avoidance-challenge/data*, accessed: 2020-07-01
2. Kazemi A. A., (2019). High Speed Laser Based Inter-satellite Link Systems for Harsh Environment of Space, *Journal of Lasers, Optics & Photonics*
3. Benzi E., Troendle D., Shurmer I., James M., Lutzer M., Kuhlmann S., (2016). Optical Inter-Satellite Communication: the Alphasat and Sentinel-1A in-orbit experience, *14th International Conference on Space Operations*
4. Carrizo C., Knapek M., Horwath J., Diaz Gonzalez D., Cornwell P., (2020). Optical inter-satellite link terminals for next generation satellite constellations, *Proc. SPIE 11272, Free-Space Laser Communications XXXII*, **1127203**
5. Lewis H. G., Maclay T., Sheehan JP., Lindsay M., (2019). Long-Term Environmental Effects of Deploying the OneWeb Satellite Constellation, *70th International Astronautical Congress (IAC)*.
6. Lewis H., Radtke J., Rossi A., Beck J., Oswald M., Anderson P., Bastida Virgili B., Krag H., (2017). Sensitivity of the Space Debris Environment to Large Constellations and Small Satellites , *7th European Conference on Space Debris*
7. Johnson N.L., Krisko, P., Liou, J.-C., Anz-Meador, P., (2001). NASA's new breakup model of evolve 4.0, *Advances in Space Research.*
8. Radtke J., Kebschull C., Stoll E., (2017). Interactions of the space debris environment with mega constellations - Using the example of the OneWeb constellation, *Acta Astronautica*, **131**, 55–68
9. Sánchez-Ortiz N., Belló-Mora M., Klinkrad H., (2006). Collision avoidance manoeuvres during spacecraft mission lifetime: Risk reduction and required Δv, *Advances in Space Research*, **38**, 2107–2116
10. Wertz J. R., Larson W. J., (1999). *Space Mission Analysis and Design*, Microcosm Press and Kluwer Academic Publishers, ed. 3
11. OKAPI:Orbits, *https://okapiorbits.space*, accessed: 2020-09-04